PHYSICAL REVIEW B VOLUME 44, NUMBER 14 1 OCTOBER 1991-II

Dynamics in spin glasses

M. Lederman and R. Orbach
Department of Physics, University of California at Los Angeles, Los Angeles, California 90024

J. M. Hammann, M. Ocio, and E. Vincent
Département de Physique, Service de Physique du Solide et de Résonance Magnétique, Centre d'Etudes Nucleaires de Saclay, 91191 Gif-Sur-Yvette CEDEX, France

(Received 11 March 1991)

Below the freezing temperature T_g, the configuration space of spin glasses is characterized by the existence of quasidegenerate equilibrium states whose number increases drastically as the temperature is lowered. The observed time dependence of the dynamical properties (aging effects) can be understood as the trend of the system towards thermal equilibrium between all accessible states. We present a series of temperature cycling experiments on the time decay of the remanent magnetization in Ag:Mn(2.6 at. %). The results are consistent with the picture of an ultrametric organization of the metastable states, predicted by the Parisi solution of the Sherrington-Kirkpatrick model. Within this interpretation, the temperature dependence of the height of the barrier between two states is determined experimentally. We also establish a quantitative relationship between the barrier height $\Delta_{\alpha\beta}$ and the Hamming distance $d_{\alpha\beta}$ separating two metastable states α and β. This experimental result is compared with numerical simulations on mean-field spin glasses.

I. INTRODUCTION

The nature of the dynamics of spin glasses has received a great deal of attention in the literature, both from experimental as well as theoretical points of view. Two theoretical perspectives have dominated. On the one hand, the mean-field approach of Sherrington and Kirkpatrick[1] (SK) and its replica symmetry solution by Parisi[2,3] has been applied in the thermodynamic limit ($N \rightarrow \infty$) to an ordered infinite set of response times.[4] On the other hand, the phenomenological approach of the droplet model, based on theories developed for the random-field Ising model (RFIM),[5-7] has been applied to the aging and time decay of the thermoremanent magnetization (TRM). We shall present, in this paper, a series of experiments which show the consistency of the aging phenomenon within an ultrametric organization of metastable states,[8] the latter predicted by the Parisi solution.[9] Within this interpretation, we shall experimentally establish a quantitative relationship between the barrier height $\Delta_{\alpha\beta}$ and the Hamming distance $d_{\alpha\beta}$ separating any two metastable states α and β.[10] We shall compare these results with numerical simulations[11,12] on mean-field spin glasses, thereby establishing a quantitative link between experiment and theory for spin-glass dynamics.

The paper is organized as follows. In Sec. II, we introduce the concept of aging in spin glasses from the waiting time dependence of the thermoremanent magnetization relaxation. In Sec. III, we introduce our interpretation of dynamics within the Parisi solution.[3] In particular, we review the consequences of an ultrametric (hierarchical) tree for the metastable (energy minima) states. We recall a series of experiments performed by Refregier *et al.*[8] which have already been analyzed along these lines. We then present a set of experiments which give further support to the hierarchical picture. In Sec. IV, we show how one can measure the temperature dependence of the height of a given barrier between two metastable states if an ultrametric organization of these states is present.[13] The procedure follows from the hierarchical nature of the evolving free-energy landscape in configuration space as the temperature is lowered. Finally, in Sec. V, we obtain experimentally a quantitative relationship between the barrier height $\Delta_{\alpha\beta}$ and the Hamming distance $d_{\alpha\beta}$ between metastable states α and β. Experimentally realizable time scales limit $d_{\alpha\beta}$ to only a few percent of phase space. Within this volume, $\Delta_{\alpha\beta}$ is shown to grow exponentially with increasing $d_{\alpha\beta}$. This functional form for $\Delta = f(d)$ will be compared with the predictions of numerical simulations by Nemoto[11] and Vertechi and Virasoro.[12] Our results are summarized in Sec. VI.

II. AGING IN SPIN GLASSES

Two properties appear necessary for a physical system to exhibit spin-glass behavior: (a) frustration (the interaction between spins is such that no configuration can simultaneously satisfy all bonds and minimize the energy at the same time, see Fig. 1) and (b) randomness (the spins must be positioned randomly in the sample). These two properties lead to highly degenerate free-energy landscapes.

Experimentally, the prototypical spin glasses are dilute magnetic alloys formed from a noble metal host (Cu, Ag, Au) and a magnetic impurity (Fe, Mn). In such systems, the exchange interaction between spins is mediated by the conduction electrons. The indirect coupling which results is known as the Ruderman-Kittel-Kasuya-Yosida

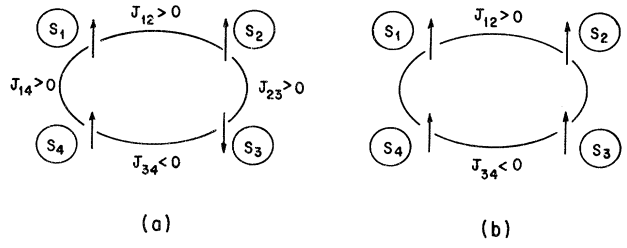

FIG. 1. Frustration effect: Energies of configurations I and II are the same. No matter in which direction spin $\mathbf{S}_3$ points, it cannot satisfy all bonds and minimize the energy at the same time.

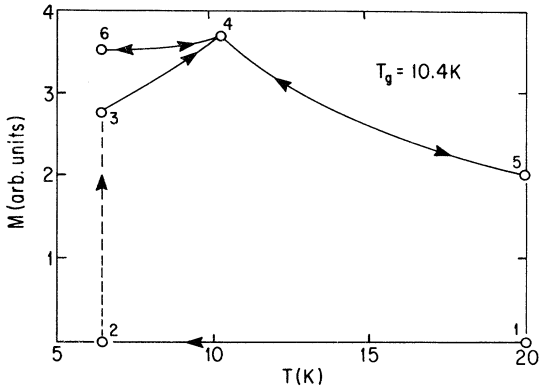

FIG. 2. Typical magnetization vs temperature measuring cycle for a Ag:Mn(2.6 at.%) sample in a field H. Cycle $1\rightarrow2\rightarrow3\rightarrow4\rightarrow5$ corresponds to a zero-field-cooled (ZFC) procedure. When 2 is reached, the external field is applied. Cycle $5\rightarrow4\rightarrow6$ corresponds to a field-cooled (FC) procedure where the sample is cooled in a field. T_g is the temperature T at which the maximum of the magnetization occurs for a given field upon ZFC. It is also the temperature where the FC magnetization becomes roughly T independent (branch $4\rightarrow6$).

(RKKY) interaction,[14] the range dependence of which is given, in $d=3$, by

$$J(\mathbf{r}_{ij}) \propto \frac{\cos(\mathbf{k}_F\cdot\mathbf{r}_{ij})}{|\mathbf{r}_{ij}|^3} , \tag{1}$$

where $\mathbf{r}_{ij}=\mathbf{r}_i-\mathbf{r}_j$, r_i and $\mathbf{r}_j$ being the spatial positions of spins i and j, and $\mathbf{k}_F$ the Fermi wave vector of the conduction electrons. Because of the oscillating term in the numerator of Eq. (1), this interaction can be either ferromagnetic or antiferromagnetic depending on the distance between spins. Combined with randomness, the RKKY interaction results in frustration. In the experiments to be presented below, the sample used was Ag:Mn(2.6 at.%) (the same sample as in Ref. 15) unless stated otherwise.

Insulating spin glasses can also exist. Typically, they are formed from magnetic compounds diluted with a nonmagnetic element. Frustration arises, for example, from ferromagnetic near-neighbor bonds together with next-near-neighbor antiferromagnetic bonds. A review of the material science aspect of the problem can be found in Ref. 16.

The universal signature of systems exhibiting spin-glass behavior is the magnetic susceptibility χ at low fields, shown in Fig. 2. When the sample is field cooled (FC), protocol $5\rightarrow4\rightarrow6$ in Fig. 2, $\chi_{\rm FC}$ becomes temperature independent below the glass temperature T_g. When a zero-field-cooled (ZFC) procedure is followed, protocol $1\rightarrow2\rightarrow3$ in Fig. 2, $\chi_{\rm ZFC}$ exhibits a cusp at T_g. The difference $\chi_{\rm FC}-\chi_{\rm ZFC}$ is the irreversible part of the magnetization. As long as the field remains constant in the spin-glass phase ($T<T_g$), the magnetization $M(H,T)$ is essentially constant, independent of time. However, if the spin-glass sample is cooled in a field down to a temperature $T_0<T_g$, and one waits a time t_w prior to cutting the field to zero, when the field is switched off, one observes a thermoremanent magnetization which decays in time. The decay of the TRM *depends* on t_w.[17] Therefore, the field-cooled state is not the equilibrium state of a spin glass. The remanent magnetization immediately after switching off the field decreases substantially as T_g is approached (see Fig. 3).[18] We refer to experiments at a fixed temperature T_0 as conventional TRM decay experiments.

As can be seen in Fig. 3, the time decay of the TRM slows down as t_w, the time spent in a field below T_g, increases. Though there is no satisfactory theory for the form of the TRM time decay, we shall make use of it as a signature of the initial state just before the field is cut to zero. This aging or memory effect is observed to speed up as the glass temperature T_g is approached.[19] The aging in spin glasses, and the reason why the system tends to reach equilibrium faster as T_g is approached, are the issues to be discussed in the next sections.[20]

III. DYNAMICS ON THE HIERARCHICAL TREE

A. Justification of the use of ultrametricity

The solution of the SK spin glass proposed by Parisi[3] generates a large number of pure states characterized by an overlap function $q_{\alpha\beta}$ between any two states α and β,

$$q_{\alpha\beta}=\left[\frac{1}{N}\right]\sum_i \mathbf{m}_i^\alpha\cdot\mathbf{m}_i^\beta . \tag{2}$$

Here, $\mathbf{m}_i^\alpha$ is the thermal average of the magnetization at site i in state α, and N is the total number of spins. For simplicity, we shall restrict ourselves to Ising spins in the remainder of this manuscript. Our sample is Ising-like for small magnetic fields ($H<380$ Oe) as shown by Fert *et al.*[21] The self-overlap $q_{\alpha\alpha}$ is the Edwards-Anderson order parameter $q_{\rm EA}$,[22] whose temperature dependence is exhibited in Fig. 4. It is clear that

$$-1\le -q_{\rm EA}(T)\le q_{\alpha\beta}\le q_{\rm EA}(T)\le 1 . \tag{3}$$

Parisi showed[3] that the set of $\{q_{\alpha\beta}\}$ is in fact a continuous function $q(x)$ (at $H=0$), from $-q_{\rm EA}$ to $q_{\rm EA}$, with x a

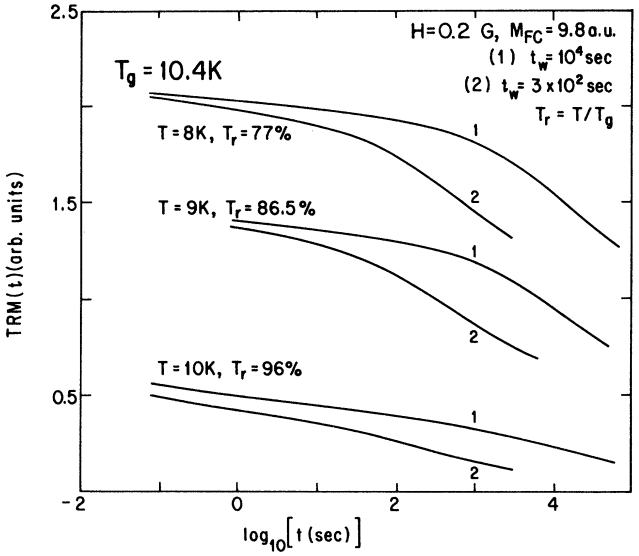

FIG. 3. Thermoremanent magnetization (TRM) decay of a sample of Ag:Mn(2.6 at.%) ($T_g=10.4$ K) cooled in a field $H=0.2$ Oe, at three different reduced temperatures $T/T_g=0.77$, 0.865, 0.96. Curves (1) and (2) correspond to waiting times $t_w=10^4$ sec and 3×10^2 sec, respectively. It is observed that the relaxation rate decreases with increasing waiting time and decreasing temperature. In particular, close to the glass temperature T_g, aging effects tend to disappear (Ref. 36).

probability defined between 0 and 1. Because of the symmetry of the problem, it is sufficient to consider the range $0\le q(x)\le q_{\rm EA}$. The quantity $q(x)$ is a multivalued order parameter for the infinite-range SK spin glass.

The number N_S of metastable states, or equivalently the number of relative minima of the free energy can also be computed.[23(a)–(c)] They correspond to the number of solutions to the TAP equations.[24] For an Ising spin glass close to T_g, N_S increases exponentially with decreasing T, or with increasing $t=1-T/T_g$:[23(c)]

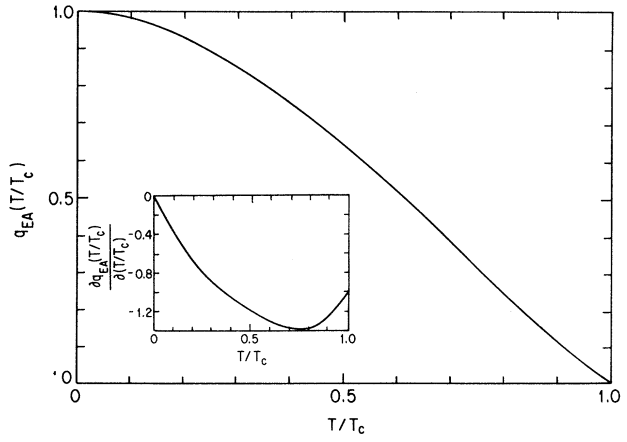

FIG. 4. Temperature variation of $q_{\rm EA}(T)=q(x=1)$ (taken from Ref. 35), where $T_g=1$. In the inset, the temperature variation of $\delta q_{\rm EA}/\delta T$ vs t ($t=T/T_g$) is represented.

$$N_S=\exp[(8/81)Nt^6]\ . \tag{4}$$

As a consequence, the complexity of the free-energy landscape in configuration space increases markedly as T is lowered. A typical experimental sample contains $N=10^{20}$ spins, so that, for $t=0.1\%$, $N_S=\exp(10)$, but for $t=1.0\%$, $N_S=\exp(10^7)$. The existence of a very large number of states suggests the existence of a very complex phase space. This will be shown to result in a wide spectrum of activation energies (energy barriers) separating these states. If the system is to reach internal thermal equilibrium upon cooling below T_g, all the barriers must be surmounted because of the ultrametric relationship between states (see discussion below). We shall show that this is possible only extremely close to T_g. Otherwise, the size of the phase space and the height of the barriers is such that one cannot expect to reach equilibrium during experimentally accessible time scales.[19]

The structure of the organization of the metastable (pure) states[25] was studied in detail in Refs. 9 and 26. The authors showed that any three states α, β, and γ having mutual overlaps $q_{\alpha\beta}$, $q_{\alpha\gamma}$, and $q_{\beta\gamma}$ obey a property called ultrametricity: at least two of the three overlaps are equal and the third is larger than or equal to the other two.[9] This property can be translated mathematically into a treelike organization of the states α, β, and γ.[10] In Fig. 5, we have constructed an ultrametric tree with the vertical axis corresponding to the overlap function $q(x)$. In this arrangement, in order to find the overlap $q_{\alpha\beta}$ between those (pure) states α and β associated with free-energy minima labeled α and β, one need only find the closest common ancestor to α and β and "read" the value of q at that level of the tree. The higher one has to move up the tree, the smaller the value of q. Equivalently, the larger the number of spins pointing in opposite directions between α and β, the smaller $q_{\alpha\beta}$. Thus, $q_{\alpha\beta}$ is a measure of the "resemblance" between states α and β, equivalent to Eq. (2).

A property shown in Ref. 26 is that all the pure states in the same hierarchical (ultrametric) tree have the same magnetization. This is why the magnetization, and hence the susceptibility in the Parisi solution, is temperature independent for $T<T_g$. The ultrametric tree is completely

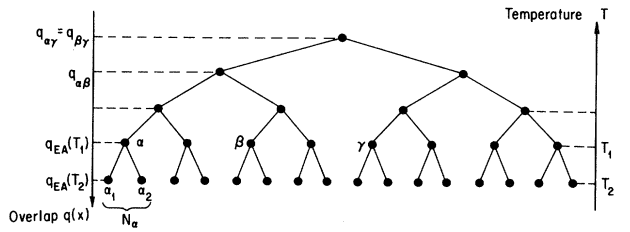

FIG. 5. Ultrametric (hierarchical) organization of metastable states at two temperatures T_1 and T_2 ($T_1>T_2$). At T_1, α, β, and γ are metastable states (relative minima of the free energy in configuration space). As observed, the mutual overlaps $q_{\alpha\beta}$, $q_{\alpha\gamma}$, and $q_{\beta\gamma}$ are such that $q_{\alpha\gamma}=q_{\beta\gamma}<q_{\alpha\beta}$. As the temperature is lowered from T_1 to T_2, state α gives "birth" to N_α states which are the new metastable states at T_2. $q_{\rm EA}(T)$ denotes the maximum value of the overlap function at temperature T.

specified once the field H (and therefore the magnetization) and the total number of spins N are defined. If a tree is constructed for all metastable states at $T=0$ (where $q_{EA}=1$), the tree at a given temperature T_0, $0<T_0<T_g$, is the same, except that the lower branches corresponding to $q>q_{EA}(T_0)$ are removed.

This construction can be interpreted physically by starting from the high end of the temperature scale, T_g. As the temperature is lowered from, say, T_1 to T_2 ($T_g \geq T_1 \geq T_2$), a given metastable state α at T_1 gives "birth" to N_α new states at T_2. These new states are the metastable states at T_2. Conversely, if the temperature is raised from T_2 to T_1, the N_α states will merge into the single state α at T_1. This is pictured in Fig. 5.

B. Experiments of Refregier *et al.* (Ref. 8)

Refregier *et al.* performed two classes of experiments on an insulating spin glass[8] which clearly showed how a hierarchical organization of metastable states can explain, in a simple manner, the dynamics observed in their samples. In the first class, the sample was field cooled to a temperature T_0. After a waiting time t_{w_1}, the temperature was *lowered* to T_1 and kept there for t_{w_3}. The temperature was then raised back to T_0, and after a time t_{w_2}, the external field was cut to zero and the TRM decay subsequently measured. It was observed[8] that, if the amplitude of the temperature step $dT=T_0-T_1$ was not too small, the relaxation was identical to the conventional TRM decay at T_0 after a waiting time $t_w=t_{w_1}+t_{w_2}$. The system apparently remained *frozen* (did not age) while being held ("waiting") for t_{w_3} at T_1. In the second class of experiments by Refregier *et al.*,[8] the sample was again field cooled to T_0. After a waiting time t_{w_1}, the temperature was *raised* to T_1 for a short time, and then cooled back to T_0. After a time t_{w_2} at T_0, the field was cut to zero and the decay of the TRM measured. It was shown[8] that, if the temperature increase, dT was larger than a certain (small) value, the relaxation of the TRM was almost indistinguishable from the TRM decay at T_0 after a waiting time t_{w_2}. Thus, only a small increase in temperature was sufficient to *reinitialize* the aging process at T_0. It is important to note that, in both classes of experiments, a minimum temperature step was required to remain frozen or to reinitialize, respectively.

These results were discussed in terms of an ultrametric (hierarchical) organization of the metastable states. In Fig. 6, we represent at each level (corresponding to a different temperature) the free-energy surface (following the approach of Dotsenko[27]). The horizontal axis corresponds to the different metastable states at the given temperature. Now, according to this hierarchical arrangement, we can make the plausible physical assumption that the smaller the overlap between states α and β (the more reversed spins between them), the higher will be the energy barrier between them because a larger number of spins must be flipped. This will be true on the average, with exceptions not very probable.

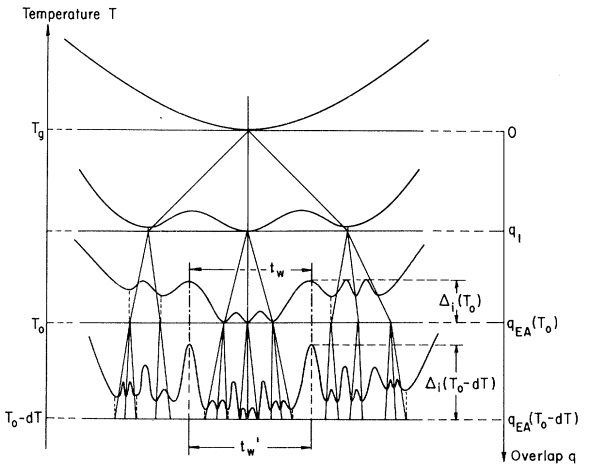

FIG. 6. Hierarchical organization of metastable states. The coarse-grained free-energy surface is represented at each level corresponding to a given temperature. When the temperature is decreased, each valley subdivides into others. The times t_w and $t_{w'}$ which are necessary to explore, at T_0 and T_0-dT, respectively, the region of phase space bounded by the same barriers are indicated. The closest common ancestor to all states within the space bounded by Δ_i at T_0 and T_0-dT is the same, and its corresponding value of the overlap function is q_1. The sketch also shows that, as the system explores more of phase space, it encounters ever increasing barrier heights, and that the free-energy surface has a self-similar structure.

Then, within the context of an ultrametric organization of metastable states, aging as well as the experiments previously described can be understood as follows. The system is cooled down to a temperature T_0, populating a single or small number of states. As it ages for a time t_w, it distributes its population among more and more states by overcoming ever increasing energy barriers. This is pictured in Fig. 6. If we suppose that the system jumps over a a barrier via a thermally activated process, then after a time t_w, the explored subspace is characterized by a highest barrier

$$\Delta_{\max}(T_0,t_w)=T_0\ln(t_w/\tau_0)\ , \tag{5}$$

where τ_0 is a microscopic attempt time.

The first class of experiments, $T_1=T_0-dT$, $dT>0$, can then be described in the following manner. After waiting at T_0 for a time t_{w_1}, a certain number of metastable states are populated. As the temperature is lowered to T_1, those states give "birth" to new ones (see Fig. 6). During the subsequent waiting time t_{w_3}, the system is populating the new metastable states. It is a much slower process than at T_0 because (a) the temperature is lower and (b) the height of a given barrier increases rapidly with decreasing temperature (this result will be proven in Sec. IV). The second factor will turn out to be the most important. If, after the waiting time t_{w_3}, the system is unable to populate more than the descendant states of

those which have been populated at T_0 after a total time t_{w_1}, the metastable states will merge into their ancestors as the temperature is raised back to T_0, thereby erasing the aging process at T_1.

The second class of experiments, $T_1 = T_0 + dT$, $dT > 0$, can also be interpreted using this approach. The states populated during t_{w_1} at T_0 will merge into fewer ones or eventually a single one as the temperature is raised (depending on the magnitude of the temperature rise). In particular, if the temperature T_1 is such that $q_{EA}(T_1) \leq q_1$, where q_1 is the value of the overlap function of the closest common ancestor to all states populated during t_{w_1} at T_0 (see Fig. 6), then one expects that the aging that occurred during t_{w_1} would be completely erased because all the states have merged into a single parent. As T is lowered back to T_0, aging restarts.

We can summarize the previous results in the following way. If a spin glass is cooled to a temperature $T_0 < T_g$, a short positive temperature step will reset the aging process. A negative temperature step will not modify the aging process. This experimental observation is well described by an ultrametric organization of metastable states.

C. Temperature cycling experiments: Influence of a temperature step and waiting time on the TRM decay

In order to further test the validity of the ultrametric organization of metastable states and to get a more quantitative picture of the continuous ramification of phase space as the temperature is decreased, we have carried out a series of TRM decay experiments. In these experiments, the system ages at a temperature $T_0 \pm dT$ ($dT > 0$) and, prior to cutting off the field, the temperature is lowered or raised to T_0. As an example, the TRM decays at $T_0 = 9.0$ K are exhibited in Figs. 7 and 8 (for $T_0 - dT$ and $T_0 + dT$, respectively). A sample of Ag:Mn(2.6 at. %) ($T_g = 10.4$ K) was used.

We present in Fig. 7 the results of a class of experiments where the sample is field cooled to $T_0 - dT$ ($T_0 = 9$ K, $H = 0.2$ Oe). After a waiting time $t_w = 3 \times 10^3$ sec, the temperature is raised to T_0 and the field is subsequently cut to zero. The decay of the TRM is then recorded. Four different values of dT were used: 20 mK (△), 40 mK (□), 60 mK (◇), and 80 mK (▲). The solid lines represent the relaxation corresponding to conventional TRM decay measurements at T_0 after waiting times $t_w = 3 \times 10^2$, 10^3, 3×10^3, and 10^4 sec. In particular, it is observed that aging at $T_0 - 40$ mK for a time $t_w = 3 \times 10^3$ sec, and aging at T_0 for $t_w = 10^3$ sec have identical TRM relaxations.[28] This property will be used in Sec. IV to evaluate the temperature dependence of the height of a specific barrier $\Delta(T)$. Our main observations are (a) the larger the temperature step dT, the shorter the waiting time at T_0 necessary to obtain the same TRM relaxation,[29] and (b) for $dT \leq 60$ mK, the shape of the TRM relaxation using the temperature cycle described above is the same as that of a conventional TRM at T_0, with an appropriate waiting time. This is at least true in our experimental time range and within our experimental resolution. (A dc Squid magnetometer is used in the measurements.) However, for $dT \geq 80$ mK, the TRM relaxation curve cannot be superposed onto one obtained in a conventional experiment. This is valid independently of how long one waits at $T_0 - 80$ mK.

The results of a second class of experiments are

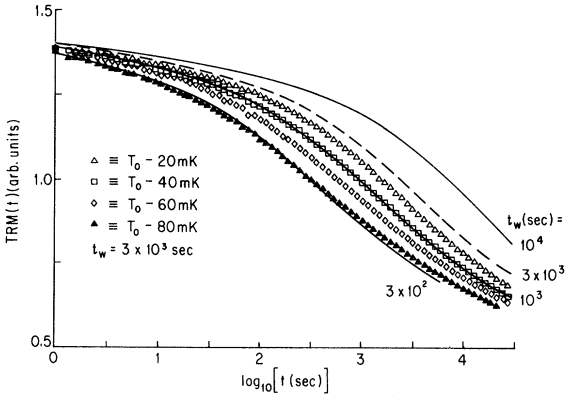

FIG. 7. Effect of aging in a field ($H = 0.2$ Oe) at $T_0 - dT$ and measuring the time decay of the TRM, for different dT. The solid lines correspond to the conventional TRM decay at $T_0 = 9$ K, with waiting times $t_w = 3 \times 10^2$, 10^3, 3×10^3, and 10^4 sec. The data were obtained by field cooling to $T_0 - dT$ [$dT = 20$ mK (△), 40 mK (◇), 60 mK (□), and 80 mK (▲)], and waiting for $t_w = 3 \times 10^3$ sec before switching off the field and measuring the time decay of the TRM. The resulting relaxations can be compared to reference relaxations at T_0 with effective waiting times decreasing with increasing dT.

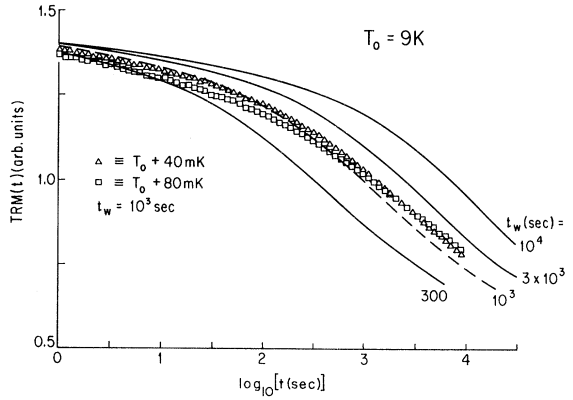

FIG. 8. Effect of aging in a field ($H = 0.2$ Oe) at $T_0 + dT$ and measuring the time decay of the TRM at T_0 for different dT. The data correspond to $dT = 40$ mK (△) and 80 mK (□), after waiting in a field for $t_w = 10^3$ sec. The solid lines correspond to conventional TRM decays at $T_0 = 9$ K, with waiting times $t_w = 3 \times 10^2$, 10^3, 3×10^3, and 10^4 sec. The relaxations obtained using the temperature cycling procedure described above cannot overlay the conventional TRM decay at T_0. See text for discussion of this point.

presented in Fig. 8. The sample is now field cooled to T_0+dT, $dT>0$. After a time $t_w=10^3$ sec, the temperature is lowered to T_0, the field is removed immediately after, and the decay of the TRM is subsequently measured. Two different dT's are presented: 40 mK (△) and 80 mK (□). We represent with solid lines the relaxation corresponding to classical TRM decay measurements at T_0, with waiting times $t_w=3\times10^2$, 10^3, 3×10^3, and 10^4 sec. This second class of experiments exhibit the following features: (c) for short observation times, the observed TRM decays lie below the $t_w=10^3$ sec conventional reference curve, and (d), for large observation times, the curves are above.[30] The larger the dT, the more amplified are observations (c) and (d).

The above observations can be described, again, in a very simple way using the hierarchical organization of metastable states presented in Sec. III A. In the first class of experiments where the sample ages at a temperature T_0-dT, the complexity of the free-energy landscape is higher, and the aging process slower, relative to that at T_0. Thus as dT increases, the region of phase space populated during a given fixed waiting time at T_0-dT is bounded by barriers whose height at temperature T_0 decreases (see Fig. 6). From Eq. (5), this implies that the effective waiting time at T_0 decreases with increasing dT [observation (a)]. In the discussion above, it was assumed that the thermal weight of a state and its descendants remains unchanged when compared with a reference state and its descendants at the corresponding temperature. This assumption may only be true as a first-order approximation. This can be seen as follows. Let N_1 states be populated at temperature T_0-dT. As the temperature is raised to T_0, that number decreases to N_0 (see Fig. 6). Immediately after T_0 is reached, the system will be in equilibrium within the populated subspace if the thermal weight of each one of the N_0 states is equal to the relative weight of their descendants at T_0-dT. As dT gets larger, this approximation becomes less valid. Thus, in the first class of experiments described above (aging at T_0-dT), the TRM decay, for large dT, corresponds to a *combination* of the normal continuation of phase-space exploration at T_0 and a reequilibration within the subspace populated while waiting in a field at T_0-dT. Therefore, the shape of the decay will differ from the conventional TRM decay at T_0, regardless of waiting time [observation (b)].

The second class of experiments can also be described following the approach of Sec. III A. The sample is now field cooled down to T_0+dT. After a time t_w, N_1' metastable states are populated at that temperature. As the temperature is lowered to T_0, each one of those states gives "birth" to new ones (see Fig. 5). Thus, when the field is cut to zero and the decay of the TRM measured, the shape of the decay will reflect two processes. First, at short times the system populates the states created by lowering the temperature. This is a fast process because it corresponds to populating states very close in phase space (large overlap) or, similarly, states separated by very small barriers [compared to $\Delta_{\max}(T_0,t_w)$]. Thus, the decay of the TRM is faster than in a conventional experiment [observation (c)]. Second, at long times, it populates the region of phase space not populated immediately after cooling from T_0+dT to T_0. In the previous section, it was shown that, the higher the temperature, the faster the aging process. Therefore, for a fixed waiting time t_w at T_0+dT, the larger the dT, the longer it takes the system, at T_0, to begin to explore states in the second stage of the time-evolution process. This is the reason why, as dT increases, the system seems to have aged more at large observation times than it would have for a time t_w at temperature T_0: the TRM decay is slower at long observation times than the reference one at T_0 with the same waiting time [observation (d)].

Thus, as in Sec. III B, the results presented in this section can be nicely explained in the context of an ultrametric organization of metastable states. It is observed that it is possible to find a time t_w such that aging at temperature T_0-dT for a time $t_{w'}$ is equivalent to aging at T_0 for a time t_w (as long as dT is small). This is not possible when aging at T_0+dT. The first of these two properties will be used in the next section.

IV. TEMPERATURE DEPENDENCE OF BARRIER HEIGHTS

In this section, we exploit the temperature cycling procedure of Sec. III C in order to obtain a direct measurement of the temperature dependence of the height of a given barrier Δ. We will extract from our measurements $(\delta\Delta/\delta T)$ as a function of Δ.

The procedure comprises two steps. First, the sample is cooled in a field $H=0.2$ Oe to a temperature T_0. After a waiting time t_w, the field is cut to zero and the decay of the TRM is measured (see solid lines in Fig. 7). Next, the system is cooled in the same field from above T_g down to T_0-dT $(dT>0)$, with $dT\ll T_g,T_0$. After a waiting time $t_{w'}$, the temperature is raised to T_0, the field is immediately switched off, and the decay of the TRM subsequently measured. In this procedure, the times t_w and $t_{w'}$ are chosen so that both decays of the TRM are identical. This was shown to be possible in Sec. III C for small enough dT.

Using the interpretation of aging given in Sec. III, we can give a physical interpretation to these experiments. In both cases, just before switching off the field, the temperature and field are the same. By choosing t_w and $t_{w'}$ appropriately, the TRM decays can also be made the same. Therefore, the region of phase space populated just before the field is cut to zero must be the same. This region of phase space can be characterized by the largest barrier overcome during the aging process, given according to Eq. (5) by,

$$\Delta(T_0,t_w)=T_0\ln(t_w/\tau_0) \tag{6a}$$

at T_0, and

$$\Delta(T_0-dT,t_{w'})=(T_0-dT)\ln(t_{w'}/\tau_0) \tag{6b}$$

at T_0-dT. Substracting (6b) from (6a) for small dT, one obtains

$$\Delta(T_0,t_w)-\Delta(T_0-dT,t_{w'})=(\delta\Delta/\delta T)_{T=T_0}dT \tag{7}$$

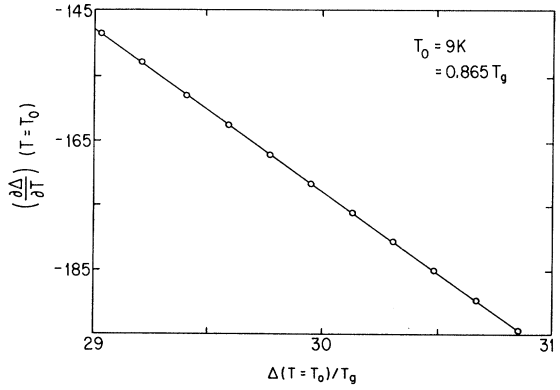

FIG. 9. Plot of $\delta\Delta/\delta T$ vs Δ at the reduced temperature $T_r = T_0/T_g = 0.865$ for the Ag:Mn(2.6 at. %) ($T_g = 10.4$ K) sample. It is found that $|\delta\Delta/\delta T|$ increases linearly with increasing Δ, and can be expressed by $(\delta\Delta/\delta T)_{T=T_0} = -a(T_0)\Delta + b(T_0)$. All quantities are given in units of T_g.

as a function of $\Delta = \Delta(T_0, t_w)$. By choosing different values of t_w, different barriers can be probed. This procedure would normally be very time consuming, but the trick of Ref. 13 was used to shorten the measurement time, leaving the nature of the experiment the same.

In Fig. 9, we present the results obtained at $T_0 = 9$ K ($T_g = 10.4$ K) for the range of barriers that can be explored within laboratory time scales (all quantities are expressed in units of T_g). We set $\tau_0 \sim 10^{-12}$ sec, in accordance with the T_g of our sample. Within the small range of Δ explored, $(\delta\Delta/\delta T)$ is well approximated by a linear function of Δ and can be expressed as

$$(\delta\Delta/\delta T)_{T=T_0} = -a(T_0)\Delta + b(T_0) , \tag{8}$$

where $a(T_0)$ and $b(T_0)$ are two positive constants depending only on T_0.[31] They are exhibited in Figs. 10 and 11, respectively, for four measurement temperatures $T_0 = 8$, 9, 9.5, and 10 K. We sketch in Fig. 6 how a given barrier evolves between T_0 and $T_0 - dT$. That figure implies that $\Delta(T_0 - dT) > \Delta(T_0)$. The results summarized in Eq. (8) prove this relation, and further show that the larger the barrier, the faster it grows with decreasing temperature. Our results, Eq. (8), are consistent, in the range of Δ explored by us experimentally, with an exponential growth of barrier height with decreasing temperature. This shows why aging slows down so markedly upon lowering T,[17] and increases in rate so rapidly upon increasing T.[19] A numerical integration of Eq. (8) should, in principle, give $\Delta(T)$. However, the rate of increase of barrier height Δ with a significant drop in temperature is so great that large barriers cannot be probed during laboratory time scales [see Eq. (5)]. At a given T, we are limited to that narrow range of $\Delta(T)$ for which t_w appearing in Eq. (5) lies within laboratory accessibility. This means that unless Eq. (8) can be extended experimentally to a larger range of Δ, we cannot determine how a particular barrier height changes over the full range of temperatures $0 \le T \le T_g$.

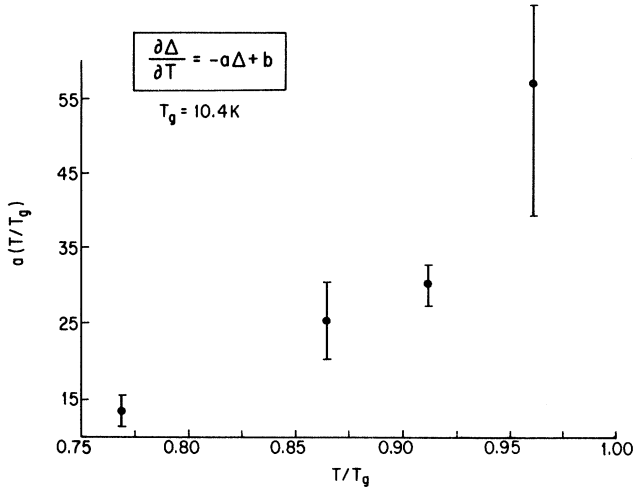

FIG. 10. Values of $a(T)$ extracted from Fig. 9 given for the four reduced temperatures $T_r = T_0/T_g = 0.769$, 0.865, 0.913, and 0.952. The error bars are determined by the procedure used when computing $\lim_{\delta T \to 0} \delta\Delta/\delta T$ (see Ref. 13).

V. BARRIER HEIGHT AND HAMMING DISTANCE

We introduced in Sec. III the concept that the free-energy landscape becomes more complex in a hierarchical fashion as the temperature is lowered. In particular, the number of metastable states grows rapidly with decreasing temperature.[23(c)] Physically, this implies that the maximum distance between states in the subspace encompassed by a given barrier at temperature T increases as the temperature is reduced. The Hamming distance is a measure of the difference between metastable states, and therefore proportional to the size of the region of phase space[10] which separates these states. The Hamming distance between two states α and β, $d_{\alpha\beta}$, is given

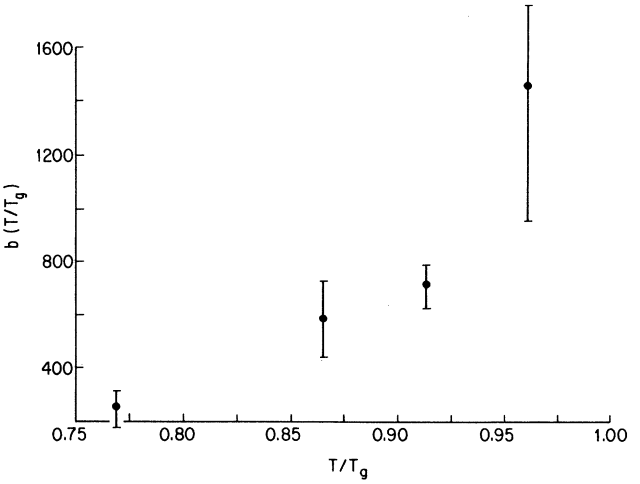

FIG. 11. Values of $b(T)$ for the same temperatures as in Fig. 10.

by[10]

$$d_{\alpha\beta}=(1/4N)\sum_i (m_i^{\alpha}-m_i^{\beta})^2=\tfrac{1}{2}(q_{\rm EA}-q_{\alpha\beta}) . \quad (9)$$

The prefactor $\frac{1}{2}$ is chosen so that the size of phase space is 1 at $T=0$ and zero at $T=T_g$ ($-q_{\rm EA}\le q_{\alpha\beta}\le q_{\rm EA}$).[32]

From Fig. 6, we see that the Hamming distance explored at temperature T_0 during a wait time t_w is given by

$$d(T_0,t_w)=(1/2)[q_{\rm EA}(T_0)-q_1] , \quad (10a)$$

where q_1 is the value of the overlap function corresponding to the closest common ancestor to the populated states. According to the protocol presented in Sec. IV, the Hamming distance at temperature T_0-dT explored within the same barriers is

$$d(T_0-dT,t_{w'})=\tfrac{1}{2}[q_{\rm EA}(T_0-dT)-q_1] , \quad (10b)$$

where q_1 is the same as in (10a) since the closest common ancestor remains the same. Equations (10a) and (10b) give the Hamming distance of the space bounded by the same barrier at the two temperatures T_0 and T_0-dT. If $dT\ll T_g,T_0$, upon substracting Eq. (10b) from Eq. (10a), one finds

$$\frac{d(T_0,t_w)-d(T_0-dT,t_{w'})}{dT}=(\delta d/\delta T)_{T=T_0}$$
$$=\tfrac{1}{2}(\delta q_{\rm EA}/\delta T)_{T=T_0} . \quad (11)$$

Equation (11) shows how the Hamming distance evolves with temperature. In the Parisi solution, $q_{\rm EA}$ corresponds to the self-overlap (overlap between a state and itself). In terms of the multivalued order-parameter function $q(x)$, $q_{\rm EA}=q(x=1)$. We have plotted $q_{\rm EA}$ and $(\delta q_{\rm EA}/\delta T)$ as a function of temperature in Fig. 4. Combining Eqs. (8) and (9), we obtain

$$\left[\frac{\delta\Delta/\delta T}{\delta d/\delta T}\right]_{T=T_0}=\left[\frac{\delta\Delta}{\delta d}\right]_{T=T_0}$$
$$=2\left[\frac{\delta\Delta}{\delta q_{\rm EA}}\right]_{T=T_0}$$
$$=\alpha(T_0)\Delta-\beta(T_0) , \quad (12)$$

for the range of Δ we explore experimentally. In Eq. (12), $\alpha(T_0)$ and $\beta(T_0)$ are positive constants, dependent only on temperature. They are equal to $2a/(\delta q_{\rm EA}/\delta T)$ and $2b/(\delta q_{\rm EA}/\delta T)$, respectively, where a and b are defined in Eq. (8). Integration of Eq. (12) gives

$$\Delta(d)-\beta/\alpha=[\Delta(d_0)-\beta/\alpha]\exp[\alpha(T)(d-d_0)] , \quad (13)$$

where d_0 and d are the Hamming distances between states separated by barriers of height $\Delta(d_0)$ and $\Delta(d)$, respectively, at temperature T. In order to appreciate the implications of Eq. (13), we have evaluated the difference in Hamming distance at $T=0.865T_g$ between the states separated by barriers of height $\Delta(t_w=10^{13}$ sec$)\simeq 30$ and $\Delta(t_w=10^4$ sec$)\simeq 32$. Using Eq. (13), one obtains $d_{32}-d_{30}=0.0068$. The maximum Hamming distance (total size of the phase space) at that temperature is $d_{\rm max}=q_{\rm EA}(0.865T_g)=0.16$. This means that, by waiting 10^4 sec instead of 10^3 sec, the increase in explored phase space is only 4.3% of the total. Clearly, time scales beyond the age of the universe would be required to reach equilibrium (explore all of phase space) even at $0.865T_g$. Because $\alpha(T)$ is an increasing function of T close to T_g [$a(T)$ increases with T and $(\delta q_{\rm EA}/\delta T)$ is almost constant], and because the maximum value of d becomes smaller as T increases, one can expect to reach thermodynamic equilibrium within experimental time scales only extremely close to the transition temperature.[19]

We have reproduced, in Fig. 12, the results obtained by Vertechi and Virasoro[12] for the theoretical relationship between barrier height and Hamming distance. They are based on numerical simulations using the Thouless-Anderson Palmer (TAP) equations[24] at T and $H=0$. One observes that, for Hamming distances $d\ge 0.5$ (at $T=0$), $\Delta(d)$ saturates. That is because this region of d corresponds to the time-reversal states. For small d ($d<0.2$), we plot $\ln\Delta$ as a function of d in Fig. 13.[33] The result is of the form $\Delta=0.13\exp(11.4d)$, qualitatively the same as that which we extracted from our experiments in Eq. (13). That the prefactor of d inside the exponential is not the same from experiment $\alpha_{\rm exp}(0.865T_g)\simeq 38.1\pm 9.5$ and theory $\alpha_{\rm thy}(OT_g)\simeq 11.4$ is most probably a consequence of the different sizes of the experimental ($N\simeq 10^{20}$) and the numerical simulation ($N=96$) samples, and the difference in temperatures. Notice also that the absolute values of the barrier corresponding to a given Hamming distance from experiment [$\Delta(d=0.0068)\sim 32$ and theory [$\Delta(d=0.04)\sim 0.2$] are not the same. We attribute this difference to the size dependence of barrier heights. Indeed, Vertechi and Virasoro show[12] that the relation $\Delta=f(d)$ is size dependent. Confirming this experimentally would be a very important result. The static Parisi

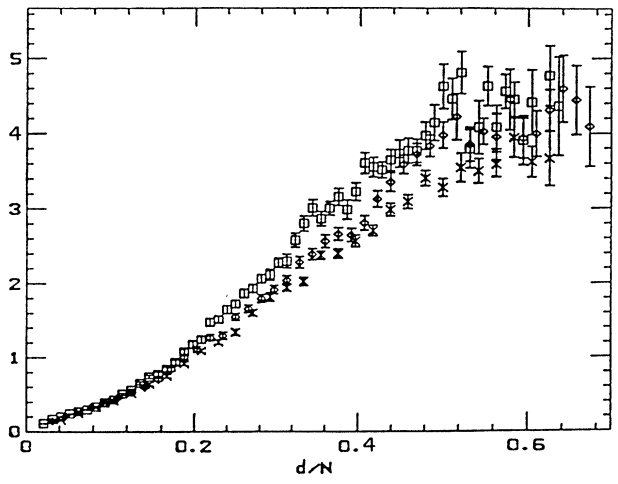

FIG. 12. Numerical simulation by Vertechi and Virasoro (Ref. 12) giving the relation between barrier heights Δ and Hamming distances d, at T and $H=0$, for spin-glass samples of different sizes $N=48$ (+), 64 ($\Diamond$), and 96 ($\Box$).

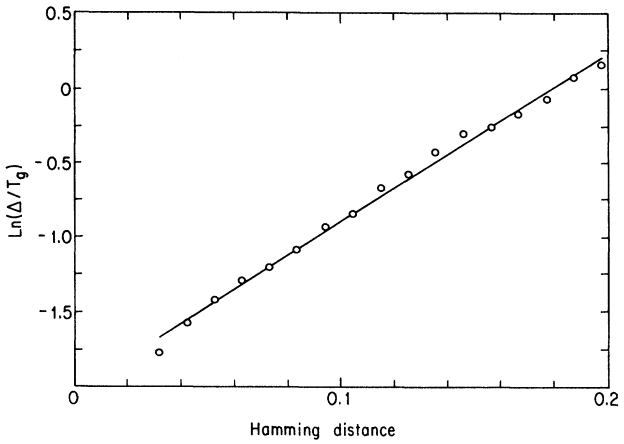

FIG. 13. Plot of $\ln\Delta$ vs d for $0.025 \leq d \leq 0.2$, where Δ and d where determined for a sample of $N=96$ (Ref. 29). The data are compatible with an exponential increase of Δ with distance d, as found from experiment [see Eq. (13)].

solution separates the pure states by infinite barriers[4] in the thermodynamic ($N \to \infty$) limit. Therefore, infinite-time scales[34] would be necessary to observe aging effects. The fact that, experimentally, we use a very large, but nevertheless finite, sample, could explain why dynamics within laboratory macroscopic time scales are observed at all.

VI. CONCLUSION

From a new set of temperature cycling experiments on a canonical spin-glass Ag:Mn(2.6 at. %), we have confirmed that the dynamic properties of spin glasses can be interpreted in terms of an ultrametric (hierarchical) organization of metastable states. Aging can be understood as the system populating more and more of phase space by hopping over barriers which increase in height as the Hamming distance between the initial and final states gets larger (the overlap between states gets smaller). We show experimentally that a given barrier increases its height very rapidly as the temperature T is lowered. Therefore, we can explain why dynamics slow down so very rapidly with decreasing temperature. Finally, a quantitative relation between a barrier height Δ and its corresponding Hamming distance d is established experimentally. It is qualitatively the same as that obtained from numerical simulations on mean-field spin glasses, establishing a link between experiment and theory of spin-glass dynamics. In the range of barriers that can be explored during experimental time scales, Δ increases exponentially with d. As suggested in Sec. V, Δ should also be an (increasing) function of the number of spins N. In particular, in Ref. 12, it is proposed that $\Delta \propto N^{\alpha}$ with $\alpha = 0.34 \pm 0.08$. Physical samples of different sizes could test this. For example, our results suggest that, for mesoscopic-size systems, equilibrium may be reached for any $0 < T < T_g$ within laboratory time scales. It is also possible that, for some insulating spin glasses, the effective N is smaller. This may indicate why aging disappears, for instance, in $Eu_{0.40}Sr_{0.60}S$ for $T \geq 0.86 T_g$.[35,37]

ACKNOWLEDGMENTS

We would like to thank M. Mezard, D. Vertechi, and M. A. Virasoro for very fruitful discussions. We thank R. Gerard-Deneuville and F. Winnykamen for their technical assistance. One of the authors (M.L.) would like to thank the SPSRM at Saclay for their kind hospitality. This research was supported in part by NSF Grant No. DMR-86-18968 and ONR Contract No. ONR-N00014-88-K-0058.

[1] D. Sherrington and S. Kirkpatrick, Phys. Rev. B **17**, 4384 (1978).
[2] G. Parisi, Phys. Lett. **73A**, 203 (1979); Phys. Rev. Lett. **43**, 1574 (1979); J. Phys. A **13**, L115 (1980).
[3] G. Parisi, Phys. Rev. Lett. **50**, 1946 (1983).
[4] This question is extensively discussed by M. Mezard, G. Parisi, and M. A. Virasoro, in *Spin Glass Theory and Beyond* (World-Scientific, Singapore, 1987). A general discussion on hierarchically constrained dynamics can be found in R. G. Palmer, D. L. Stein, E. Abrahams, and P. W. Anderson, Phys. Rev. Lett. **53**, 958 (1984). More particular studies can be found in C. P. Bachas and B. A. Huberman, J. Phys. A **20**, 4995 (1987), and in K. H. Hoffman and P. Sibani, Z. Phys. B **80**, 429 (1990), who study the particular case of spin-glass dynamics in an ultrametric tree.
[5] A. J. Bray and M. A. Moore, Phys. Rev. Lett. **58**, 57 (1987).
[6] G. Koper and H. Hilhorst, J. Phys. (Paris) **49**, 429 (1988).
[7] D. S. Fisher and D. A. Huse, Phys. Rev. B **38**, 373 (1988).
[8] Ph. Refregier, E. Vincent, J. Hammann, and M. Ocio, J. Phys. (Paris) **48**, 1533 (1987).
[9] M. Mezard, G. Parisi, N. Sourlas, G. Toulouse, and M. A. Virasoro, J. Phys. (Paris) **45**, 843 (1984).
[10] R. Rammal, G. Toulouse, and M. A. Virasoro, Rev. Mod. Phys. **58**, 765 (1986).
[11] N. Nemoto, J. Phys. A **21**, L287 (1988).
[12] D. Vertechi and M. A. Virasoro, J. Phys. (Paris) **50**, 2325 (1989).
[13] M. Lederman, R. Orbach, J. Hammann, and M. Ocio, J. Appl. Phys. **69**, 5234 (1991).
[14] M. A. Ruderman and C. Kittel, Phys. Rev. **96**, 99 (1954); T. Kasuya, Prog. Theor. Phys. **16**, 45 (1956); K. Yosida, Phys. Rev. **106**, 893 (1957).
[15] M. Alba, M. Ocio, and J. Hammann, Europhys. Lett. **2**, 45 (1986).
[16] D. Chowdury, *Spin Glasses and Other Frustrated Systems* (Princeton University, Princeton, NJ, 1986).
[17] R. V. Chamberlin, Phys. Rev. B **30**, 5393 (1984); R. Hoogerbeets, Wei-Li Luo, and R. Orbach, Phys. Rev. B **34**, 1719 (1986).
[18] P. Norblad, P. Svendlindh, L. Lundgren, and L. Sandlund, Phys. Rev. B **33**, 645 (1986).
[19] Wei-Li Luo, M. Lederman, R. Orbach, N. Bontemps, and R.

Nahoum, Phys. Rev. B **41**, 4465 (1990).

[20]A recent review of the dynamics of spin glasses can be found in J. Ferre and N. Bontemps, Mater. Sci. Forum **50**, 21 (1989).

[21]A. Fert and P. M. Levy, Phys. Rev. Lett. **44**, 1852 (1981); N. de Courtenay, H. Bouchiat, H. Hurdequint, and A. Fert, J. Phys. (Paris) **47**, 1507 (1986).

[22]S. F. Edwards and P. W. Anderson, J. Phys. F **5**, 965 (1975).

[23](a) C. De Dominicis, M. Gabay, T. Garel, and H. Orland, J. Phys. (Paris) **41**, 923 (1980); (b) F. Tanaka and S. Edwards, J. Phys. F **10**, 2471 (1980); (c) A. J. Bray and M. A. Moore, J. Phys. C **13**, L469 (1980).

[24]D. J. Thouless, P. W. Anderson, and R. G. Palmer, Philos. Mag. **35**, 593 (1977).

[25]In Ref. 9, the only configurations of the system being considered are the so-called "pure states." They are a subset of all possible metastable states (relative minima of the free energy), and correspond to those states whose difference in free energy with respect to the ground state is of the order of N^0, where N is the number of spins. Therefore, in the thermodynamic limit (SK model), only the pure states have a nonzero thermal weight. Furthermore, it can be shown that they are separated by infinite barriers (Ref. 4). In an experimental sample, composed of a finite number of spins, the distinction between a pure state, and any relative minimum of the free energy that may not be a pure state as $N\rightarrow\infty$, cannot be made because all metastable states have a finite, nonzero, thermal weight. Therefore, in this paper, we shall suppose that all metastable states are organized according to Refs. 9 and 26. This includes states separated by finite barriers. We argue that this is plausible because, as will be shown in Sec. III B as the temperature is lowered a given pure state produces new ones (see Fig. 5). These additional pure states were some of the "old" metastable states. But because the "additional" pure states are organized ultrametrically as described in Refs. 9 and 26, this means that when they were metastable states (at a higher temperature), there was also an underlying hierarchical organization among them.

[26]M. Mézard and M. A. Virasoro, J. Phys. (Paris) **46**, 1293 (1985).

[27]V. S. Dotsenko, J. Phys. C **18**, 6023 (1985).

[28]By stating that the two sets of parameters ($T_0, t_w = 10^3$ sec) and ($T_0 - 40$ mK, $t_w = 3.10^3$ sec) have "identical TRM relaxations," we mean that when superposing the two TRM decays, they lie on top of one another to within our accuracy and in our measurement time range: $1 < t < 5.10^4$ sec. Our statement is based only from data obtained in our measurement time frame, and it is only valid for small temperature steps dT (see Fig. 7).

[29]P. Granberg, L. Sandlund, P. Norblad, P. Svendlindh, and L. Lundgren, Phys. Rev. B **38**, 7097 (1988).

[30]P. Granberg, L. Lundgren, and P. Norblad (unpublished).

[31]This relation is valid only in the range of barriers explored at T_0. It is seen in Sec. V that the phase space probed during experimental time scales is a small fraction of the total available phase space. Thus, Fig. 9 may only correspond to the tangent to the curve $(\delta\Delta/\delta T) = f(\Delta)$. Its functional form may be more complex. We remark also that Eq. (8) becomes unphysical for $\Delta < \Delta_0 = b/a$. Δ_0 corresponds to a time ~ 1 sec [See Eq. (5)]. This is due to the realization of the experiment which requires a temperature step which takes ~ 1 sec to accomplish. This observation gives a lower bound to the barriers that can be probed experimentally.

[32]The definition given for the Hamming distance is valid only for an Ising system. For vector spins, a proper definition for the Hamming distance (Ref. 10) between states α and β is $d^2_{\alpha\beta} = (1/4N)\sum_i |\mathbf{m}_i^\alpha - \mathbf{m}_i^\beta|^2$.

[33]The results of the simulation giving $\Delta = f(d)$ for $0.025 \leq d \leq 0.2$ were communicated to us by D. Vertechi and M. A. Virasoro.

[34]N. D. Mackenzie and A. P. Young, Phys. Rev. Lett. **49**, 301 (1982).

[35]N. Bontemps and R. Orbach, Phys. Rev. B **37**, 4798 (1988).

[36]Wei-Li Luo, Ph.D. thesis, UCLA, 1989.

[37]K. Binder and A. P. Young, Rev. Mod. Phys. **58**, 801 (1986).